Chemical and Biological Sensing through Optical Resonances in Microcavities

Melikhan Tanyeri[1], Mikaela Nichkova[2] Bruce D. Hammock[2, 3] and Ian M. Kennedy[†4],
[1]Department of Physics, [2]Department of Entomology, [3]Cancer Research Center, [4]Department of Mechanical and Aeronautical Engineering and Biomedical Engineering Graduate Group,
University of California, Davis, CA 95616

ABSTRACT

A microdroplet or a latex microsphere often acts as an optical cavity that supports Morphology Dependent Resonances (MDRs) at wavelengths where the droplet circumference is an integer multiple of the emission wavelength. Enhanced radiative energy transfer through these optical resonances can also be utilized as a transduction mechanism for chemical and biological sensing. Enhancement in radiative energy transfer is observed when a donor/acceptor pair is present in the resonant medium of a microcavity. Here, we demonstrate avidin-biotin binding and its detection through a FRET pair as a potential application for ultra-sensitive detection for fluoroimmunoassays. The binding interaction between the biotinylated fluorescent beads (donor) and streptavidin-Alexa Fluor 555 (acceptor) conjugate was used to observe the energy transfer between the dye pairs. Strong coupling of acceptor emission into optical resonances shows that the energy transfer is efficiently mediated through these resonances.

Keywords: Fluorescence, MDRs, microdroplet, FRET, quenching

1. INTRODUCTION

Recent studies have shown that optical resonances, often called Whispering Gallery Modes (WGMs) or Morphology Dependent Resonances (MDRs), can be used for biomolecule detection[1-6]. For example, protein detection has been demonstrated by the shift of the resonant spectrum in a silica microsphere through the adsorption of proteins on to the microsphere, changing its optical properties resulting in a sensitive detection scheme[5]. It is also possible to detect single bacterial cells in microdroplets -at cell concentrations as low as one per droplet- through observing changes in the optical resonances due to the local refractive index change and scattering caused by the cells[6].

One of the most common optical detection techniques used for bioassays is fluorescence detection. Some of these techniques use an affinity based energy transfer phenomenon called Fluorescence Resonance Energy Transfer (FRET). A non-radiative energy transfer occurs between a donor and an acceptor depending on the distance between them and the overlap of the emission spectrum of the donor and the excitation spectrum of the acceptor. The transfer efficiency depends inversely on the sixth power of the distance between the donor and the acceptor molecule leading to a powerful nanoscale (2-10 nm) measurement technique. The transfer efficiencies for a wide variety of fluorescent dyes have been studied[7]. Non-fluorescent quenchers such as QSY can also be used as efficient acceptors (donors) because of their availability in a wide spectrum range and the absence of any intrinsic fluorescence emission.

FRET can be used as an efficient detection tool for fluoroimmunoassay applications[8-15]. Antibody and antigen pairs can be tagged with FRET pairs, e.g., antibody with a fluorescent dye and antigen with its FRET pair; and used in different immunoassay formats including competitive assays. The binding reaction can be observed as a simultaneous decrease in the donor signal and an increase in the acceptor signal due to the energy transfer between the fluorescent dyes when they are in close proximity. If a non-fluorescent dye (quencher) is used as an acceptor, then we only observe the decrease in the donor signal and relate it to the reaction between the antibody-antigen.

Microdroplets have several advantages for performing FRET based immunoassays[16-17]. The first advantage is the small sample volume that is presented in the micron-sized droplets used in the experiments. The second advantage

† imkennedy@ucdavis.edu; phone (530) 752-2796; fax (530) 752-4158

Imaging, Manipulation, and Analysis of Biomolecules and Cells: Fundamentals and Applications III,
D. V. Nicolau, J. Enderlein, R. C. Leif, D. L. Farkas, R. Raghavachari, eds., Proc. of SPIE Vol. 5699
(SPIE, Bellingham, WA, 2005) · 1605-7422/05/$15 · doi: 10.1117/12.588169

is the elimination of non-specific binding to the sample container walls. The droplets are airborne and only interact with laser light. Another advantage arises from the optical cavity formed by the microdroplets. The energy transfer can be enhanced due to the morphology dependent resonances captured inside the microdroplet[18]. The emission from donor molecules can be efficiently coupled to these resonant modes, enhancing the field strength at those wavelengths. The acceptor molecules can be excited through these resonances without being in the close proximity of the donor molecule, which is a general requirement for FRET. Thus a more efficient energy transfer mechanism can be established and used to detect a wide variety of binding reactions. Here, we demonstrate the detection of the specific binding of avidin and biotin through enhanced energy transfer between a FRET pair in a microdroplet.

2. EXPERIMENTAL

2.1 Experimental Setup

The experimental setup consists of a droplet generator, two lasers, a spectrometer and a CCD camera (Fig. 1). The droplet generator is a customized commercial piezo inkjet printhead, which is driven by a function generator (Agilent 33120A, Palo Alto, CA) through a specially developed circuit. One of the nozzles of the printhead is used to eject approximately 20-micron diameter droplets. A square voltage of 6.3 V p-p is sufficient to eject droplets. Increasing the magnitude of voltage applied to the piezo only changes the initial speed of the droplets and does not affect the size of the droplets. The droplets are diagnosed about 2 mm away from the orifice. The droplets reach the laser focus in a time scale of few milliseconds with an initial ejection speed on the order of few meters per second.

The droplets are first detected by a He-Ne laser (Uniphase, Manteca, CA) and a photodiode (Thorlabs, Newton, NJ). The red laser beam (633 nm) is focused on the droplets at a closer vertical position to the printhead nozzle and at a different angle than the Argon ion laser and the forward-scattered light is collected through a series of lenses and filters and focused onto the photodiode. The current induced in the photodiode is monitored through a digital oscilloscope (LeCroy, WavePro 7000, Chestnut Ridge, NJ). The peak of the signal is set as a threshold for the droplet detection and used as a timer for triggering the delay generator. Two filters were used to avoid false signals due to the strong scattering from the Argon ion laser and red fluorescence emission from Alexa Fluor 555. One of them is a shortwave cutoff filter at 540 nm (Optosigma, Santa Ana, CA). This filter can block the scattered blue light from the laser. The second filter is a narrow-band interference filter (Optosigma, Santa Ana, CA), centered at 633 nm with a bandwidth of 1 nm. This filter blocks possible emission from Fluorescein or Alexa Fluor 555 dye in the droplet, which would interfere with the scattering light from the droplets through He-Ne laser. Since we observed the spectra in the 500-620 nm range, scattering from the droplets due to elastic scattering of He-Ne light did not affect our results.

Through this configuration, the fluctuations in the vertical position of the droplets were eliminated. By observing the scattering signal from the droplets, it is possible to determine the phases of the droplet ejection including satellite droplet formation. This allowed us to probe the droplets where they are stable and spherical and set their position precisely relative to the laser beam, resulting in a dramatic improvement in repeatability.

After the detection, the droplets generated by the printhead were optically pumped by an Argon ion laser (Coherent, Innova 70, Santa Clara, CA). The original beam (1.5 mm diameter at the $1/e^2$ point) was directed through a 488 nm bandpass filter (FWHM 1 nm, Optosigma, Santa Ana, CA) and was focused to a 50-micron spot to get better coupling of the pump beam into the microdroplets.

The resultant fluorescent signal from the droplets was collected by a long working distance Plano Apochromat lens (Mitutoyo, Kawasaki, Japan); then focused through an objective lens onto a 150 mm focal length dual grating imaging spectrometer (Acton Research Corporation, SpectraPro-150, Acton, MA). The scattered laser light collected by the collection lenses was filtered by a holographic notch filter (Kaiser Optical Systems Inc., Ann Arbor, MI) at 488 nm. The spectrometer was connected to a TEK 512x512D front-illuminated thermoelectrically cooled CCD camera (Princeton Instruments, Trenton, NJ). The data were collected and processed through the Princeton Instruments software controlling the camera shutter and the controller. The camera and the droplet generator were synchronized by the function generator and the delay generator (Stanford Research Systems, DG535, Sunnyvale, CA,).

2.2 Methods and Materials

Fluorescein-labeled biotin (biotin-4-fluorescein); streptavidin-Alexa Fluor 555 conjugate (3 moles dye/mole protein); streptavidin-Alexa Fluor 610 conjugate (5 moles dye/mol protein); biotin labeled FluoSpheres (40 nm,

yellow/green fluorescent); neutravidin labeled FluoSpheres (40 nm, yellow/green fluorescent) and Alexa Fluor 555 dye were purchased from Molecular Probes (Eugene, OR). To prepare biotinylated BSA-Rhodamine conjugate, ImmunoPure biotinylated BSA (8 moles biotin/mol BSA) was purchased from Pierce (Rockford, IL). 5-carboxyrhodamine 6G, succinimidyl ester was obtained from Sigma (St. Louis, MO). BSA-biotin and BSA were labeled with Rhodamine 6G following a standard procedure recommended by Molecular Probes. The degrees of labeling obtained were 1.3 moles Rhodamine/mol BSA-biotin and 1.4 moles/Rhodamine/mol BSA. FluoSpheres are polystyrene beads, which are internally loaded with a variety of dyes. Yellow-green fluorescent beads have excitation/emission maxima of 505/515 nm and thus are excited very efficiently using the 488 nm spectral line of the argon-ion laser. Biotin conjugated beads were used to observe the binding reaction between biotin and streptavidin. Neutravidin conjugated beads were used to conduct a control experiment for avidin-biotin reaction. Small bead size (40 nm) was chosen for two reasons. First reason is to eliminate the background signal in the Alexa Fluor 555 emission range due a possible bulk fluorescence emission from the beads. The second reason is to reduce the avidin binding ratio per bead and make it closer to the 4:1 ratio as observed in avidin-biotin binding in bulk solution. All solutions were prepared with PBS buffer (8.18 g/L NaCl, 2.98 g/L KCl, 0.27 g/L $Na_2HPO_4.7H_2O$, 1.43 g/L KH_2PO_4, pH=7.5). After each run the printhead was flushed with 20 ml deionized water (DI water) (Resistance = 18 MΩ) and operated for 5 minutes to avoid contamination between each run. A Spectramax M2 microplate reader (Molecular Devices, Sunnyvale, CA) and black 96-well plates from Nunc (Rochester, NY) were used for initial FRET studies.

3. RESULTS AND DISCUSSIONS

We chose the avidin-biotin pair as a demonstration that FRET due to the high binding affinity; this combination can be used efficiently for fluoroimmunoassay applications in microdroplets. Avidin and biotin can be conjugated with different dye pairs using straightforward protocols and because of the relatively small size (biotin is a small molecule and avidin has dimensions of approximately 5.6 nm x 5.0 nm x 4.0 nm); the distances are suitable to observe energy transfer between the dye pairs. One avidin has four biotin-binding sites.

Initially, we studied the binding reaction between streptavidin and biotinylated BSA in a 96-well microtiter plate. Due to the considerable overlap of the emission spectrum of Rhodamine (absorption/emission maxima 525/547 nm) and absorption spectrum of Alexa Fluor 610 (absorption/emission maxima 612/628 nm) in the 550-600 nm range, these dyes can be used as a FRET pair to study the binding reaction between streptavidin and biotin. The degrees of labeling for the conjugates used in this experiment were 5.1 Alexa Fluor 610 molecules per one streptavidin molecule and 1.3 Rhodamine molecules per one biotinylated BSA molecule (8 moles biotin/mol BSA). Solutions prepared in PBS solution were mixed in the 5-20 μg/ml range for both reagents and incubated for at least 30 minutes before data acquisition in a fluorescence plate reader. Measurements for solutions containing only BSA-biotin-Rhodamine and only streptavidin-Alexa Fluor 610 were performed for blank subtraction. The fluorescence intensity was measured between 550 nm and 700 nm (excitation: 525 nm) and the changes in the emission spectrum of Rhodamine and Alexa Fluor 610 were observed. After the blank subtraction, this binding reaction did not show any FRET. At constant Alexa Fluor 610 concentration, Rhodamine concentration was increased from 5 μg/ml to 20 μg/ml and no substantial change (less than 10%) in Alexa Fluor 610 emission was observed. To verify these data, the experiment was repeated with a non-specific pair, replacing BSA-biotin-Rhodamine with BSA-Rhodamine (1.4 moles Rhodamine/mol BSA). Streptavidin-Alexa Fluor 610 and BSA-Rhodamine pair showed a similar spectrum with the biotinylated pair. This shows that avidin-biotin reaction did not result in FRET between the dyes. This could be due to the relatively long distance between donor and acceptor molecules due to the low donor concentration (1.3 Rhodamine molecule per BSA-biotin).

To reduce the distance between the donor and the acceptor molecule, biotin-4-fluorescein (absorption/emission maxima 495/519 nm) and streptavidin conjugated with Alexa Fluor 555 (Absorption/Emission maxima 553/568 nm) pair was chosen thus excluding BSA from the reaction. The streptavidin-Alexa Fluor 555 concentration was kept in the 0-100 μg/ml range corresponding to 0-1.76 μM. The biotin-fluorescein concentration was varied between 1.4 and 11.2 μM to keep some excess fluorescein to account for the 4:1 binding ratio. In this configuration, the donor molecule was fluorescein and the acceptor molecule was Alexa Fluor 555. Similar to the Rhodamine/Alexa Fluor 610 pair, the Fluorescein/Alexa Fluor 555 pair also has substantial overlap for their emission/absorption spectra. The labeling ratio was 3 Alexa Fluor 555 molecules per one streptavidin molecule and 1 fluorescein molecule for each biotin molecule. The fluorescence emission intensity measurements were performed in a microplate reader between 510 nm and 620 nm (excitation at 485 nm) following incubation for at least 30 min. After

the blank subtraction, the emission spectrum for both dyes were compared. We observed a major decrease in fluorescein intensity while the streptavidin-Alexa Fluor 555 concentration was increased at a constant fluorescein-4-biotin concentration (Fig. 2). When the streptavidin-Alexa Fluor concentration was above saturation, all the biotin-fluorescein molecules in the solution were bound to streptavidin and fluorescein emission intensity dropped down dramatically. But this decrease in fluorescein emission did not result in an increase in Alexa Fluor 555 emission. This means that instead of a resonant energy transfer to Alexa Fluor 555, the fluorescein emission was quenched by the binding reaction. Since the biotin-fluorescein complex is a small molecule (MW=644), the binding reaction caused static quenching by streptavidin. This was confirmed by a control experiment where biotin-fluorescein was mixed with avidin only. The same fluorescence intensity drop was observed.

To avoid physical quenching due to binding, the link between biotin and the fluorescent tag should be sufficiently long. To achieve this, we used biotinylated fluorescent beads. As noted in the Materials and Methods section, we used 40 nm biotinylated fluorescent polystyrene beads (absorption/emission maxima 505/515 nm) with streptavidin-Alexa Fluor 555 to observe FRET. The streptavidin-Alexa Fluor 555 concentration was kept in the range from 25-200 μg/ml, while the fluorescent bead concentration was changed between 0.0045% and 0.019% corresponding to $1.31\text{-}5.25 \times 10^{12}$ beads/ml. The fluorescent intensity measurements were performed at 500-620 nm (excitation at 485 nm) and emission peaks were observed with varying donor or acceptor concentration. The result was a decrease in fluorescent emission intensity from the nanobeads, corresponding to an increase in fluorescence intensity in Alexa Fluor 555 emission (Fig. 3). This increase in acceptor intensity due to a decrease in donor emission implies an energy transfer between these molecules. Unlike the biotin-fluorescein and streptavidin-Alexa Fluor 555 reaction, the donor and acceptor molecules were close enough without being affected by the avidin-biotin interaction. We performed three control experiments to confirm this observation. Initially, to check whether observed intensity changes were due to specific binding, we replaced streptavidin-Alexa Fluor 555 with Alexa Fluor 555 only. As the Alexa Fluor 555 concentration was increased at constant fluorescent bead concentration, we did not neither observe a significant decrease in fluorescence emission from the beads nor an increase in Alexa Fluor 555 emission. Additionally, we substituted biotinylated fluorescent nanobeads with beads, which were conjugated to neutravidin. In this case, we did not expect specific binding to occur between this pair. 0.1% BSA was added to the solution before incubation to reduce non-specific binding of streptavidin to the beads. As expected, fluorescence emission intensities revealed that there was no correlation between donor and acceptor emission intensities when there is no specific binding. As a final verification, we checked the reaction between the biotinylated fluorescent beads and avidin only. In this scheme, we observed whether the binding reaction affects the donor emission in the absence of acceptor molecule. The fluorescence intensity dropped less than (10% compared to 50% in FRET) compared to the case where the acceptor molecule was conjugated to avidin. This observed intensity drop for the fluorescent bead emission shows that part of the donor emission drop observed in streptavidin-Alexa Fluor 555 and biotinylated fluorescent bead reaction is due to the binding reaction itself and cannot be completely attributed to FRET between the labels.

High optical intensities in microdroplets are able to increase the energy transfer efficiency for the FRET pairs, resulting in a high sensitivity biodetection scheme. To demonstrate this effect, we repeated the biotinylated fluorescent bead and streptavidin-Alexa Fluor 555 binding reaction in microdroplets using the setup shown in Fig 1. In a microdroplet, the emission from the fluorescent beads can be coupled to the resonances inside the cavity and increase the emission lifetime. This can result in much longer Förster radii than expected for the FRET pair. The same energy transfer pattern was achieved with microdroplets with a further decrease in donor emission fluorescence and a larger increase in acceptor emission because of improved energy transfer efficiency (Fig. 4 and 5). Streptavidin-Alexa Fluor 555 concentration was kept in the 25-200 μg/ml range, while the fluorescent bead concentration was changed between 0.0045% and 0.019%. We observed the morphology dependent resonances based on the fluorescence spectrum of fluorescent beads and Alexa Fluor 555. From Figs. 3 and 4, we observe that there is some bulk fluorescence emission, which is not associated with the fluorescence resonance energy transfer. This is due to the fluorescent donor molecules located in the inner region of the beads, which are sufficiently removed from their acceptor pair to support FRET. As a result, the donor emission decreases but was not completely quenched because of the energy transfer. Reducing the bead size can reduce the bulk emission from the beads.

Some of the most important factors affecting the FRET effect due to specific binding are the number of fluorescent molecules conjugated to avidin/biotin; the ratio of the concentrations of labeled avidin/biotin; the temperature and pH of the media as it affects the fluorescence spectrum; the emission/absorption overlap of the donor/acceptor pair; and the excitation wavelength. The detection mechanism used in this work can be applied to several immunoassay formats, including a competitive fluorescence immunoassay. The antibody can be conjugated to

the donor dye of a FRET pair while the antigen can be coupled to the acceptor molecule. The initial emission from the acceptor molecule should be high because of the energy transfer between the donor and the acceptor. When an unknown amount of antigen is introduced into the solution, some of these antigens will replace the antigens labeled with the acceptor molecule and the change will be observed as a decrease in the acceptor emission.

4. CONCLUSIONS

Optical resonances in microdroplets were used to enhance the detection of binding reaction between avidin and biotin through FRET. Streptavidin and biotinylated BSA binding did not result in a non-radiative energy transfer between Rhodamine and Alexa Fluor 610. A better FRET pair selection and a higher labeling ratio (donor molecule per streptavidin) for the donor molecule may alter this conclusion. Static or contact quenching of biotin-fluorescein upon binding to avidin was observed. No significant increase in acceptor emission was observed during this interaction, which shows that the reduction in donor signal was not due to FRET but quenching. The use of a biotinylated fluorescent bead and streptavidin-Alexa Fluor 555 interaction caused a decrease in donor emission that was associated with an increase in acceptor emission. This energy transfer can be enhanced in a microdroplet because of the long photon interaction and residence time for high Q optical cavity modes. Since the fluorescence lifetime can be increased inside the microcavity and the coupled light can travel long distances around the droplet rim, a longer Forster radius is permissible and the detection limit can be improved. This detection method can be applied to a variety of immunoassay formats.

ACKNOWLEDGEMENTS

This publication was made possible by Grant 5 P42 ES04699-16 from the Superfund Basic Research Program, National Institute of Environmental Health Sciences, NIEHS. The support of NSF through Grant DBI - 02662 as part of the Nanoscale Science and Engineering program is also appreciated.

REFERENCES

1. Vollmer, F., Arnold, S., Braun, D., Teraoka, I. & Libchaber, A. DNA detection from the shift of whispering gallery modes in multiple microspheres. Biophysical Journal 84, 295a-295a (2003).
2. Vollmer, F., Arnold, S., Braun, D., Teraoka, I. & Libchaber, A. Multiplexed DNA quantification by spectroscopic shift of two microsphere cavities. Biophysical Journal 85, 1974-1979 (2003).
3. Arnold, S., Khoshsima, M., Teraoka, I., Holler, S. & Vollmer, F. Shift of whispering-gallery modes in microspheres by protein adsorption. Optics Letters 28, 272-274 (2003).
4. Vollmer, F., Arnold, S. & Libchaber, A. Novel, fiber-optic biosensor based on morphology dependent resonances in dielectric micro-spheres. Biophysical Journal 82, 161a-162a (2002).
5. Vollmer, F., Braun, D., Libchaber, A., Khoshsima, M. & Teraoka, I. Protein detection by optical shift of a resonant microcavity. Applied Physics Letters 80, 4057-4059 (2002).
6. Tanyeri, M., Kennedy, I. M. Microdroplets for integrated high-sensitivity biosensors. Proc. SPIE Vol. 5275, 133-140 (2004).
7. Marras, S. A. E., Kramer, F. R., Tyagi, S. Efficiencies of fluorescence resonance energy transfer and contact-mediated quenching in oligonucleotide probes. Nucleic Acid Research 30, e122 (2002)
8. Grant, S.A., Xu, J., Bergeron, E.J., Mroz, J. Development of dual receptor biosensors: an analysis of FRET pairs. Biosensors and Bioelectronics 16, 231-237 (2001)
9. Ko, S., Grant, S.A. Development of a novel FRET method for detection of Listeria or Salmonella. Sensors and Actuators B 96, 372-378 (2003)
10. Adamczyk, M., Moore, J.A., Shreder, K. Quenching of biotinylated Aequorin bioluminescence by dye - labeled avidin conjugates: Application to homogenous bioluminescence resonance energy transfer assays. Organic Letters 3, 1797-1800 (2001)
11. Wang, G., Yuan, J., Matsumoto, K., Hu, Z. Homogeneous time-resolved fluoroimmunoassay of bensulfuron-methyl by using terbium fluorescence energy transfer. Talanta 55, 1119-1125 (2001)
12. Zahavy, E., Fisher, M., Bromberg, A., Olshevsky, U. Detection of frequency resonance energy transfer pair on double-labeled microsphere and Bacillus anthracis spores by flow cytometry. Appl. and Environ. Microbiology 69, 2330-2339 (2003)

13. Bruno, J.G., Ulvick, S.J., Uzzell, G.L., Tabb, J.S., Valdes, E.R., Batt, C.A. Novel immuno-FRET assay method for Bacillus spores and Escherichia coli O157:H7. Biochem. and Biophys. Research Comm. 287, 875-880 (2001)
14. Santangelo, P.J., Nix, B., Tsourkas, A., Bao, G. Dual FRET molecular beacons for mRNA detection in living cells. Nucleic Acids Research 32, e57 (2004)
15. Michelini, E., Mirasoli, M., Karp, M., Virta, M., Roda, A. Development of a bioluminescence resonance energy-transfer assay for estrogen-like compound in vivo monitoring. Analytical Chemistry 76, 7069-7076 (2004)
16. Nichkova, M., Feng, J., Sanchez-Baeza, F., Marco, M.P., Hammock, B.D., Kennedy, I.M. Competitive quenching fluorescence immunoassay for chlorophenols based on laser-induced fluorescence detection in microdroplets. Analytical Chemistry 75, 83-90 (2003)
17. Feng, J., Shan, G., Hammock, B.D., Kennedy, I.M. Fluorescence quenching competitive immunoassay in micro droplets. Biosensors and Bioelectronics 18, 1055-1063 (2003)
18. Arnold, S., Holler, S., Druger, S.D. Imaging Enhanced Energy Transfer in a Levitated Aerosol Particle. Journal of Chemical Physics 104, 7741-7748(1996)

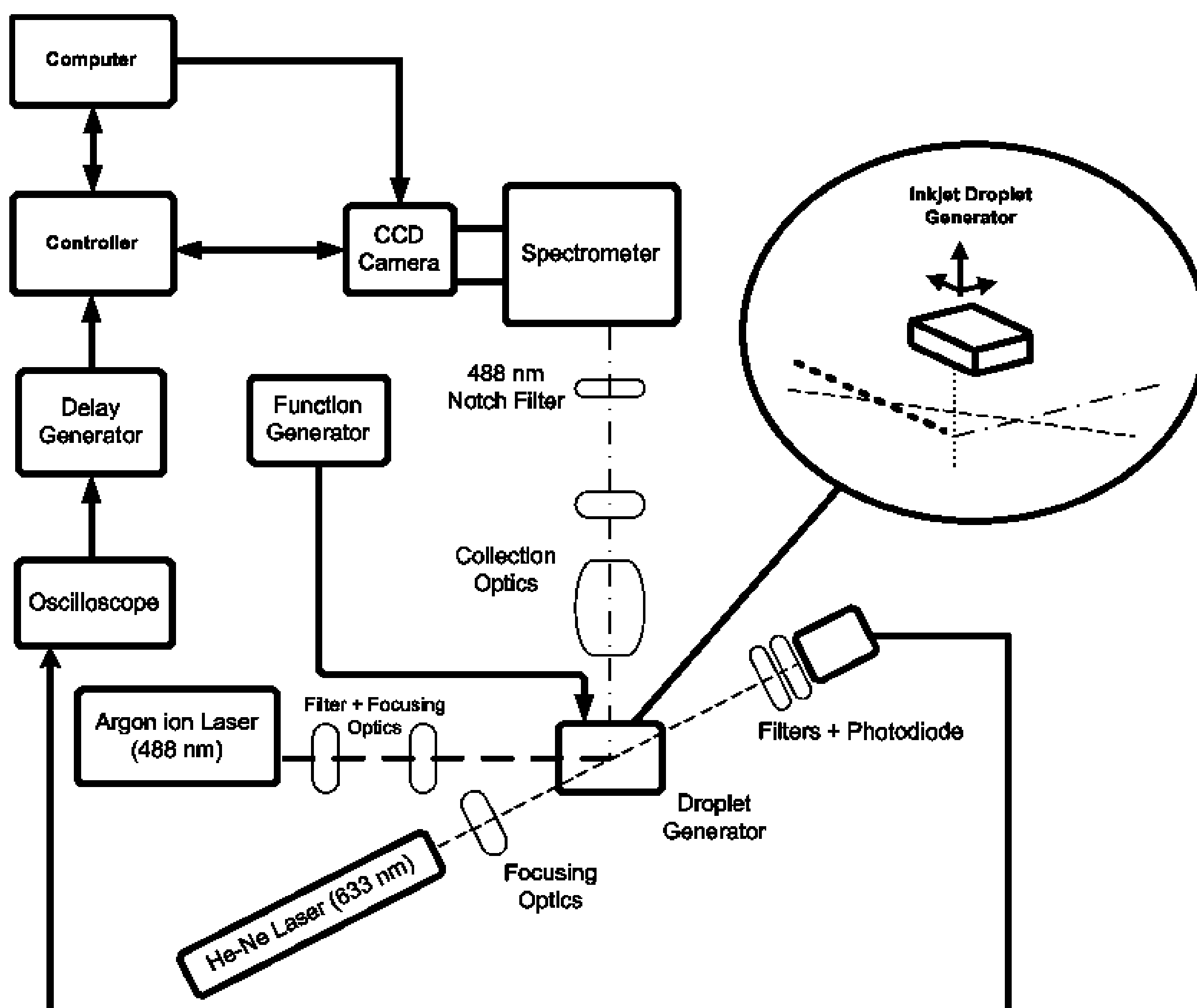

Fig. 1. Experimental setup for microdroplet lasing experiments.

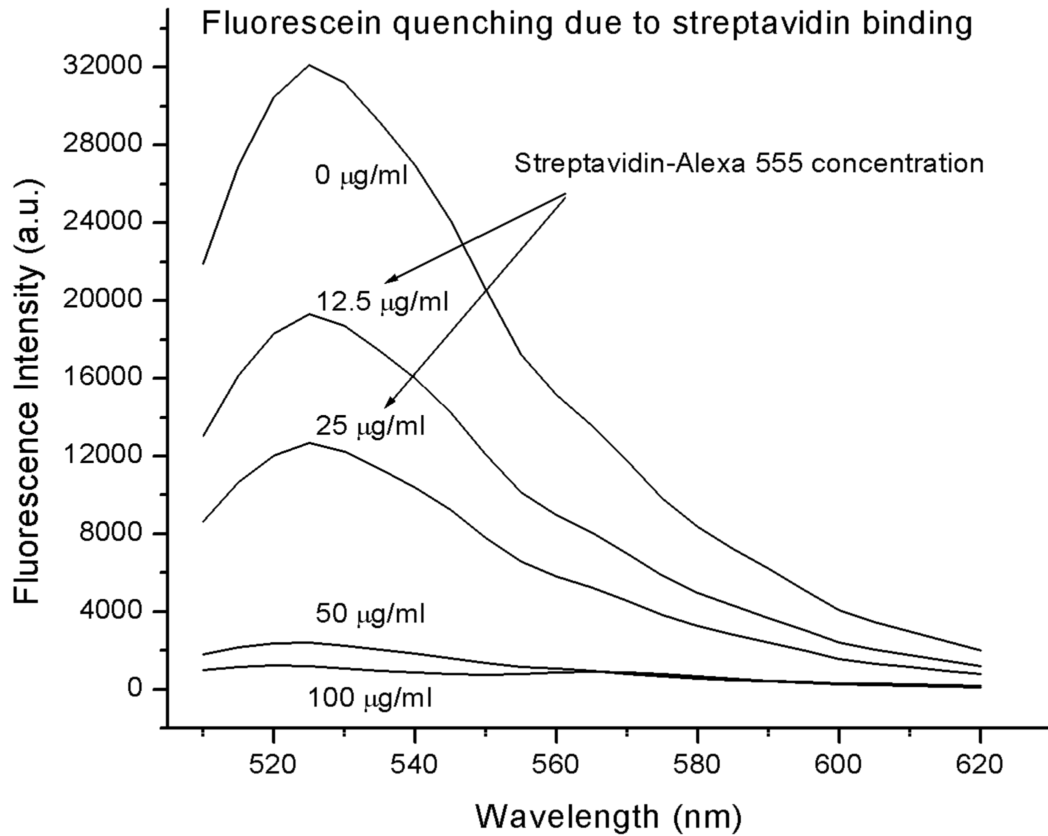

Fig. 2. Biotin-4-fluorescein (Absorption/Emission maxima 495/519 nm) and streptavidin-Alexa Fluor 555 (Absorption/Emission maxima 553/568 nm) interaction (Emission spectra at 485 nm excitation). The spectra correspond to 5.6 μM biotin-4-fluorescein at different streptavidin-Alexa Fluor 555 concentrations (0-100 μg/ml). Labeling ratio was 3 Alexa Fluor 555 (acceptor) molecules per one streptavidin molecule and 1 fluorescein (donor) molecule for each biotin molecule. A major decrease in fluorescein intensity due to contact quenching was observed when Alexa Fluor 555 concentration was increased at a constant fluorescein concentration.

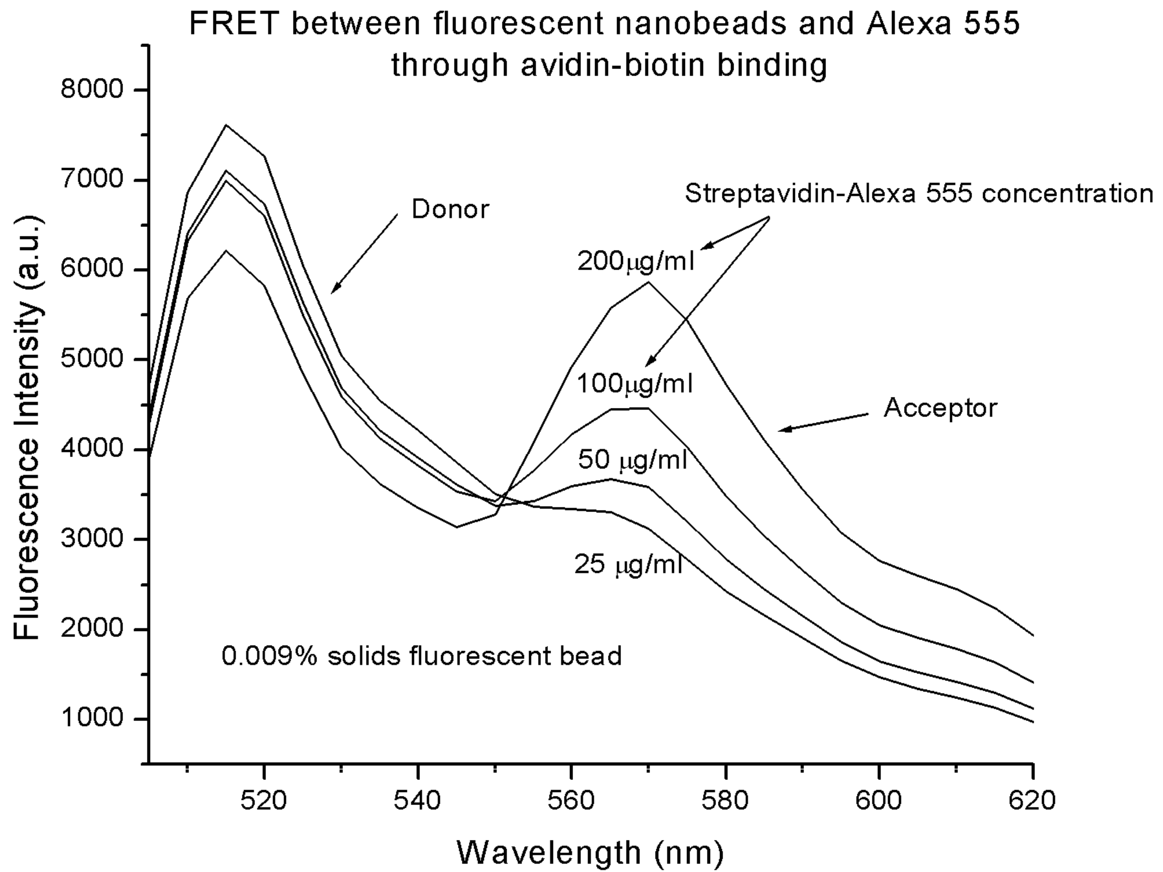

Fig. 3. 40 nm biotinylated fluorescent polystyrene beads (Absorption/Emission maxima 505/515 nm) and streptavidin-Alexa Fluor 555 interaction (Emission spectra at 485 nm excitation). The spectra presented corresponds to 0.009% solids fluorescent beads and streptavidin-Alexa Fluor 555 at various concentrations (25-200 μg/ml). A decrease in fluorescent emission intensity from the nanobeads corresponding to an increase in fluorescence intensity in Alexa Fluor 555 emission is observed. This increase in acceptor intensity due to a decrease in donor emission implies an energy transfer between these molecules.

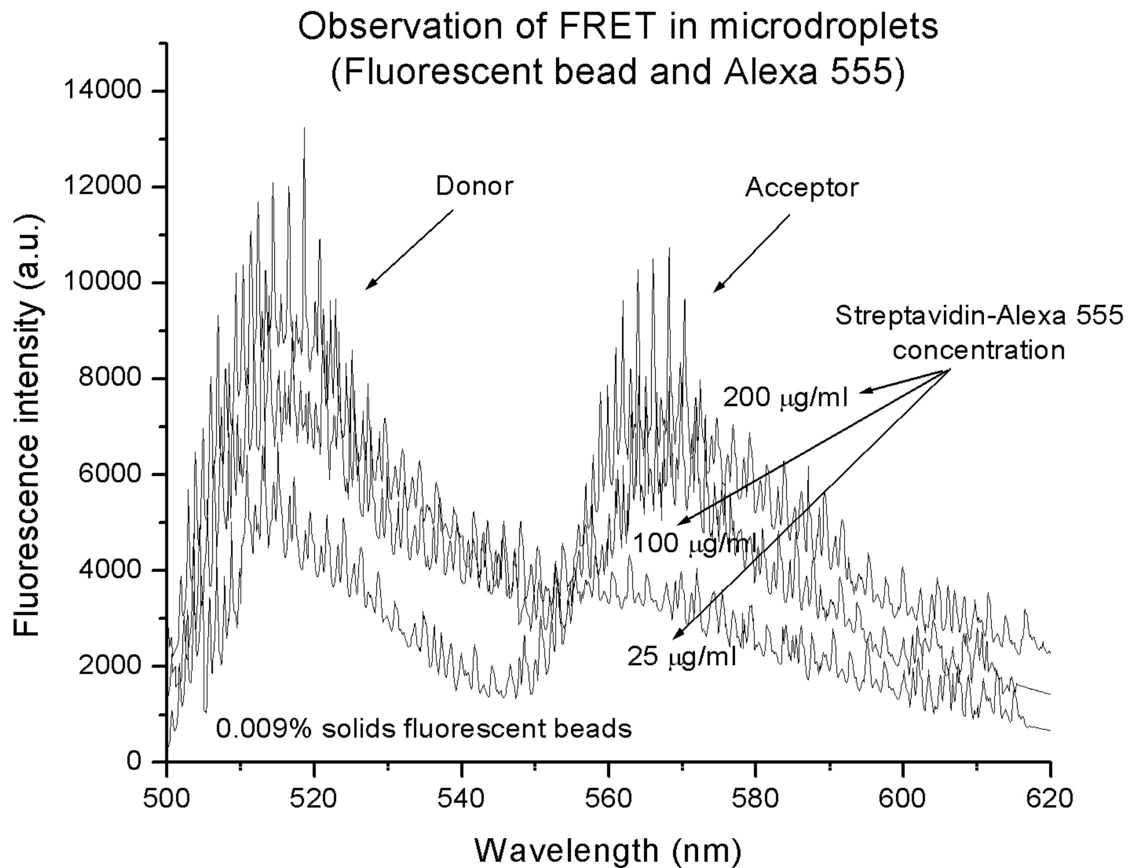

Fig. 4. Biotinylated fluorescent bead and streptavidin-Alexa Fluor 555 binding reaction in microdroplets. The spectrum presented correspond to three different streptavidin-Alexa Fluor 555 concentrations (25,100,200 µg/ml) at constant fluorescent bead concentration (0.009 % solids). As the streptavidin-Alexa Fluor 555 concentration is increased, there is a decrease in the donor (fluorescent bead) emission (500-550 nm; laser excitation at 488 nm). Morphology dependent resonances based on the fluorescence spectrum of fluorescent beads and Alexa Fluor 555 are also observed. In the microdroplet, the emission from the fluorescent beads can be coupled to the resonances inside the cavity and increase the emission fluorescence lifetime. This results in an enhanced energy transfer between donor and acceptor molecules.

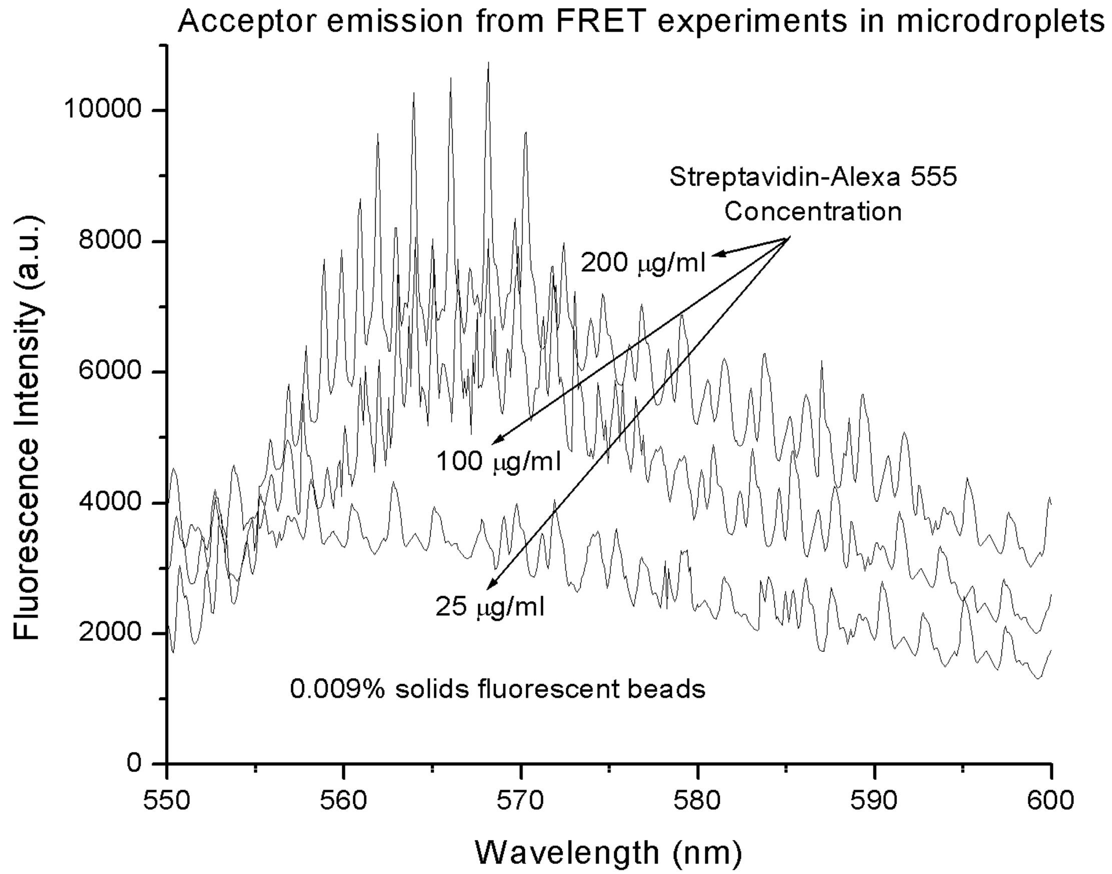

Fig. 5. Acceptor (Streptavidin-Alexa Fluor 555) emission due to donor (biotinylated fluorescent bead) excitation through FRET as a result of the specific binding reaction in microdroplets. This figure shows the acceptor emission spectra in the 550-600 nm range and it is enlarged from Figure 4.